WIDER Working Paper No. 2013/067

Characterizing wind power resource reliability in southern Africa

Charles Fant[1] and Udaya Bhaskar Gunturu[2]

July 2013

Abstract

Producing electricity from wind is attractive because it provides a clean, low-maintenance power supply. However, wind resource is intermittent on various time scales, thus introducing variability in power output that is difficult for electric grid planning. In the following study, wind resource is characterized using metrics that highlight these intermittency issues, therefore identifying areas of high and low wind power reliability in southern Africa at different time scales. After developing a wind speed profile, these metrics are applied at various heights in order to assess the added benefit of raising the wind turbine hub. Furthermore, since the interconnection of wind farms can aid in reducing the overall intermittency, the value of interconnecting near-by sites is mapped using three distinct methods. Of the countries in this region, the Republic of South Africa has shown the most …/

[1]University of Colorado Institute of Climate and Civil Systems (ICLiCS); [2]MIT Joint Program for the Science and Policy of Global Change, corresponding author email: fantcw@colorado.edu

interest in wind power investment. For this reason, we focus parts of the study on wind resource in the country. The study finds that, although wind power density is high in South Africa compared to its neighboring countries, wind power resource tends to be less reliable than in other parts of southern Africa—namely, central Tanzania and parts of Kenya. We also find that South Africa's potential varies over different time scales, with higher potential in the summer than winter, and higher potential during the day than at night. This study is concluded by introducing a variety of methods and measures to characterize the value of interconnection, including the use of principal component analysis to single out areas with a common signal.

1   Introduction

As the threat of climate change builds, there is a push towards lower emissions. One strategy for reducing emissions is to build away from carbon-intensive electricity production and toward clean energy sources like the energy produced from wind and sun. Clean energy resources are dominated by new technologies that are dependent on intermittent, locally unique sources not yet well understood. Understanding the past variability of climate in relation to potential renewable resources can steer investment towards beneficial sustainable ventures and avoid poor investment decisions. In the following section, a study is presented to better understand the future reliability of wind and solar resources based on an analysis of the historical climate state. In the last few decades there has been a growing interest in wind-generated electricity. The idea being, if planned properly, wind can provide a renewable, cost-effective long-term investment as well as a clean energy source. But, due mostly to the uncertainty caused by the chaotic characteristics of wind near the earth's surface, wind power generation is intermittent on useful operating time scales (hours and days), and likely inconsistent in the long-term (years and decades). Southern Africa provides an interesting case study for this analysis, specifically the southern Africa development countries, which includes the Democratic Republic of Congo, Tanzania, and all countries south of these two. Energy demand in this region of the world is rising quickly, with more than 12 per cent in Mozambique and more than 10 per cent in Zimbabwe, as observed in the last couple of years, for example (SAPP 2012).

1.1 Energy sector in South Africa

Of the countries in this region, South Africa has shown the most interest in wind technology investment. With 80 per cent of the electricity capacity of the Southern Africa Power Pool (SAPP; SAPP 2010), South Africa is one of the most carbon-intensive countries in the world (DEA 2011). Economic growth has been driven largely by the abundance of local coal resources, which currently satisfies about 77 per cent of South Africa's primary energy needs (DOE 2011). The accessibility of coal has resulted in a dependence on low-cost coal-fired electricity, energy-intensive mining, and heavy industry (Alton et al. 2012). Regardless, the South African government aims to reduce greenhouse gas emissions significantly, hoping to cut down on emissions by 42 per cent by 2025 compared to a business-as-usual scenario (RSA 2010) and the Department of Energy in South Africa plans to achieve 30 per cent clean energy by 2025 (DOE 2011). In order to satisfy these goals, enormous changes in infrastructure must take place. One essential change in infrastructure is a move from coal-fired electricity to electricity generated from renewable sources—namely biofuels, wind, solar, and imported hydropower. The major players in the electricity sector of South Africa are Eskom and the Department of Energy. Eskom generates approximately 95 per cent of the electricity used in South Africa and 45 per cent of the electricity used in Africa, and was converted from private to public in 2002 (Eskom 2012). With stakes in the Cohora Bassa hydroelectric scheme in Mozambique, South Africa can import 1,400 MW firm energy plus an additional 300 MW non-firm energy (Wilson and Adams 2006). Although renewable sources are occasionally used for rural areas that cannot feasibly connect to the national grid, commercially viable renewable energy capacity is not yet exploited on a large scale. Domestic hydropower capacity is small compared to other sources, less than 2 per cent of the current energy production, and has been almost fully developed (DEA 2011). There are currently three operational wind power plants in South Africa, all small scale, although there are a few large scale wind farms in planning. Sere Wind Farm, to be among the largest wind

farms, is proposed to be built near the city of Vredendal in the Western Cape (Savannah Environmental 2007).

1.2 Wind resource characterization

Wind resource study is often characterized by a time and spatial scale, which is driven by the overall purpose. Due to the relatively high inertia of wind turbines, changes in wind speed that occur on time scales less than one minute (ultra high frequency) are typically considered negligible. This sets the limit on the lower time scale extremes. Large time scales are limited by the expected life of a wind turbine, which is generally about 20 years. Therefore, useful wind resource assessment falls between a time scale of high frequency (minutes) and inter-annual frequency (years). The relevant spatial scale largely depends on the study objectives. In a project scale, or local scale study (less than 1 km), the effects of trees, buildings, and hills are significant. On larger scales, these effects can be generalized into a roughness length coefficient and aggregated over time to avoid false precision (Peterson et al. 1997).

Typically, for national planning purposes, wind resource is characterized following a few similar steps. First, an annual mean wind speed dataset is used to specify wind resource geographically. In the past, this has been a collection of wind station data, as in Diab (1995) for South Africa. Then, the estimated annual mean wind speed is used, along with assumed or estimated shape parameter(s), to represent the distribution of wind speed over time using a fitted distribution (Cavallo 1993). The Weibull distribution is most widely used (Ucar and Balo, 2009; Pryor and Barthelmie, 2010; Zaharim et al., 2009; Eskin et al., 2008, among others) because it fits wind speed distribution fairly well, reproducing the positive skewness, and only requires two parameters for fitting (Tuller and Brett 1984). Recently, some doubt has been raised about using the Weibull distribution as noted in Gunturu and Schlosser (2011). Jaramillo and Borja (2004) found that the Weibull distribution could not be generalized to two parameters for fitting some wind regimes. Morrissey et al. (2010) also found the Weibull fitting to be inaccurate for the wind speed distribution at a particular site. The study found that the Weibull fitting underestimated lower wind speed frequencies and overestimated higher wind speed frequencies. Further, buoyancy fluxes have been found by He et al. (2010) to distort typical wind behavior away from a fitted Weibull distribution. The study also found that the Weibull distribution does not reproduce the positive skewness typically observed in night time winds.

Once the typical behavior of wind is generalized, a reference wind turbine is typically used to estimate the power theoretically generated, applying the limitations of cut-in and cut-out wind speeds. Cut-in wind speed is the minimum speed at which wind turbines generate power, while cut-out speed is the maximum speed at which, for various reasons, power cannot be generated. An example of a typical power curve is shown in Figure 1 to illustrate the importance of cut-in and cut-out wind speed in power generation (Hagemann 2008).

In order to avoid the limitations of choosing a specific wind turbine, others have described the wind resource in a more generalized form. The wind power generated by wind turbines is related to the cube of wind speed (V) and air density (ρ). A common value used to express this relationship is wind power density (WPD) using the following equation

$$WPD = \frac{1}{2}\rho V^3$$

(1)

Due to the cubic relationship of wind power generated and wind speed, higher wind speeds are important to identify, both spatially and temporally. Note that, in Figure 1, the C_p coefficient represents the fraction of WPD that can be utilized by the Vestas V80. This represents the efficiency of the turbine, which reduces as wind speed increases, resulting in a relationship that is almost linear, although piecewise, with four distinct stages: no power from 0 to 4 m/s; steep increase from 4 m/s to about 14 m/s; a flat relationship from 14 m/s to 25 m/s, independent of incremental changes in wind speed; and no power produced above the cut-out wind speed of 25 m/s.

Due to recent technological advancements in wind turbines, there are more hub height options than in the past. For this reason, typical wind resource assessment requires an understanding of the changes in the potential energy generated at different hub heights. With these characterized, one can weigh calculated benefits against the marginal costs of increasing the hub-height. A common approach to estimating wind speeds at different heights is to use a power law of the form

$$\left(\frac{\overline{V_1}}{\overline{V_2}} \right) = \left(\frac{z_1}{z_2} \right)^{\alpha}$$

(2)

where V_1 and V_2 are the wind speeds at the reference location and the estimated location, respectively, and z_1 and z_2 are the heights at the reference and estimated location, respectively. This relationship is also commonly used to estimate hub height wind speeds from anemometer records near the surface. In most cases, the shear exponent (α) is assumed to be one-seventh (Elliott et al. 1987, 1991; Sailor et al. 2008, among others). Schwartz and Elliot (2005) found that the actual value of the shear exponent is considerably greater than one-seventh. They also found that windy sites tend to have lower values of α than less windy. Using a constant value, then, might result in an overestimate of wind speed at higher altitudes for less windy sites.

Wind resource mapping of South Africa

A very important intermediate step in the typical wind characterization process is mapping the resource. So far, there have been two completed, well-documented attempts to map wind resource over South Africa. Diab (1995) developed an initial wind resource map, effectively classifying areas of good, moderate, and low wind power potential. Diab used 79 long-term weather stations of varying geographic settings with classical methods estimating mean wind speed, wind power density, and Weibull distribution parameters. She also estimates mean monthly and daily wind fluctuations over the year. Diab found that a band covering the full coast of South Africa is likely to be the area where wind potential is the highest, with some moderate potential further inland. Hagemann (2003) points out a few problems with this early work, mostly in the use of the weather station data and measurement errors in the data itself. Following Diab's work, an attempt was made by Eskom and other partners in the early 2000s to develop a more reliable wind resource map. Unfortunately, these were never made available to the public (Hagemann 2008).

Hagemann produced the second wind resource map as part of his 2008 PhD dissertation. Hagemann (2008) explored the value of using the regional climate model, MM5, to develop a high-resolution wind climatology for South Africa, representing a typical year. As a result, he produced a meso-scale map of wind resource, which superseded Diab's work. Figure 2 shows Hagemann's map of mean annual wind speed at 10 m. This work has produced the most

recent full map of wind resource in South Africa. Hagemann estimates that South Africa has a total potential wind generation of about 80.5 TWh, 35 per cent of total 2007 electricity sales.

Recently, it has become popular to map wind resources using a combined meso-/micro-scale modeling technique imploring the Karlsruhe Atmospheric Mesoscale Model (KAMM; Adrian and Fiedler 1991; Adrian 1995) and the micro-scale model WAsP (Troen and Peterson 1989). WAsP makes use of the previously discussed Weibull distribution. This technique has been used in studies of Ireland, as well as Europe, Russia, and Egypt, among others (Landberg et al. 2003). A similar study began for South Africa around 2010 called the 'Wind Atlas for South Africa' (WASA), co-ordinated by the South African National Energy Development Institute, SANERI. This work, slated to finish in June 2013, has made available some initial presentations, results, and data (Szewczuk and Prinsloo 2010). One major contribution from this work was the installation of proper wind measurement towers that record wind measurements at turbine hub heights up to 63 m.

2   Data

With the advancement of satellite utility and measurements, global datasets are becoming more popular for areas with a limited or unreliable set of historical data. For this study, the MERRA (Modern-Era Retrospective for Research and Analysis) reanalysis dataset is used (Rienecker et al. 2011). The MERRA dataset is attractive because it attempts to represent a balance between satellite, station, and modeled climate gridded globally at an hourly time-step from 1979 to 2009. Although there are certainly limitations to the reanalysis approach, MERRA improves on the representation of the hydrologic cycle and uses a large repository of conventional observations from various sources, as well as satellite radiance data.

Wind speed can then be estimated using the following logarithmic empirical relationship, taking into consideration roughness length (z0), height (z), and friction velocity (u*) (Stull 1991).

$$V_z = \left(\frac{u_*}{k}\right) \ln\left(\frac{z-d}{z_0}\right) \tag{3}$$

The MERRA data provides the necessary variables for this calculation. In this equation, the wind is assumed to be neutrally stable, a common assumption in wind power assessments.

The spatial scale of MERRA is set to $1/2°$ by $2/3°$, somewhere between meso-scale and synoptic scale, and the time scale is set between hourly and inter-annual (by aggregation). One of the caveats of using data aggregated over a grid is that the aggregation could cause misrepresentations of the climate. Of course, a wind farm would be subject to the wind behavior at a much smaller spatial scale, so it is important to understand the differences between gridded (i.e. aggregated) and point (i.e. as measured from a station) climate.

3   Mapping

Using the MERRA dataset and Equation 1 to estimate wind speed at 50 m, mean wind speed is mapped to compare with Hagemann's wind atlas. Of course, Hagemann's wind atlas was produced at 10 m above ground. Figure 3 shows the mean wind speed in m/s at 50 m. These results look similar to Hagemann's in most areas in South Africa. There are higher wind

speeds in the southwest and lower in the northeast. Also, South Africa has relatively high mean wind speeds compared to its neighboring countries.

3.1 Wind power density and measures of central tendency

Mean and median WPD for southern Africa are shown in Figure 4. Any value below 50 W/m^2 is considered to have no wind power potential and is shown as white.

Similar to the map of wind speed, there is a large area around central Africa (northwest in the map) where the wind power potential is poor. This area extends over the majority of the Democratic Republic of the Congo, into northern Angola, and east to the western parts of Tanzania and Uganda. The areas of good wind resource potential are in central Tanzania, the southwestern part of South Africa, and most of Kenya. There are also some smaller areas of potential along the border of Botswana and Zimbabwe, southern Mozambique, and parts of Zambia.

Typically, mean wind speed or mean WPD is used to show the central tendency of wind resource potential. Due to the skewness of the WPD toward lower values, Gunturu and Schlosser (2012) suggest that the median is a more meaningful measure of central tendency for national grid planning. The median is especially useful because it represents what the theoretical output produced at least half of the time, providing a simplified sense of reliability. As shown in Figure 4, the median is considerably lower than the mean. In fact, the area of poor wind resource potential in the northwest portion of the map extends south over Angola and into most of Namibia. In the past, a threshold of 220 W/m^2 was used to classify poor wind resource potential (Gustavson 1979). Although that wind power technology has developed some since 1979, if a value of 220 W/m^3 were used here, one could claim that the only areas of good wind resource potential would be in the east—namely the grids in central Tanzania and Kenya.

3.2 Measures of variance

Another valuable measure of wind resource is a measure of variability. Large unpredictable changes in wind speed over time are problematic for power distribution planning. Therefore, an area with lower variability is more desirable than one with higher variability, given that they have comparable central tendencies. A useful measure of variance is the coefficient of variation (CoV), which is shown for WPD for southern Africa in Figure 5. Here, a value of 1 means that the standard deviation is the same as the mean. A value above 1 means that the standard deviation is larger than the mean and below 1 means the mean is larger than the standard deviation. In general, the areas with a larger mean WPD have lower CoV. One exception to that would be a comparison of the central area of Tanzania with the southwestern area of South Africa. These two regions have similar mean WPD but the southwestern part of South Africa has a significantly higher CoV suggesting that this area is less desirable for wind power harvesting. Another useful measure of variance is the robust coefficient of variation (rCoV) defined as

$$rCoV = \frac{median(|WPD - median(WPD)|)}{median(WPD)}$$

(4)

where WPD is a time series of wind power density values. The interpretation of rCoV is similar to that of CoV where a value of 1 means that the median absolute difference between the value and the median of the time series is equal to the median of the time series.

Therefore, a rCoV of 1 means that central tendency of the absolute difference from median of the WPD time series is greater than twice the median or zero, since WPD cannot be negative. This map also shows the striking difference between central Tanzania and southwestern South Africa. In fact, all of South Africa appears to have a highly variant WPD, even the areas where the median value is high. In terms of variance, eastern Africa proves to exhibit a better source for wind power harvesting.

3.3 Measures of reliability

To further our understanding of the quality of wind resource in southern Africa, we have decided to map two measures of reliability. First, we must choose a threshold to classify wind power for a given grid and hour as either usable or unusable. In the past, a value of 220 W/m^2 has been demonstrated as the minimum needed for wind power generation (Gustavson 1979). For this study we have chosen to follow the US Wind Resource Atlas and use a value of 200 W/m^2 to account for advances in technology (Elliott et al. 1987), which was also used in Gunturu and Schosser (2012). The first measure we calculated is availability. Availability is the number of hours with usable WPD (i.e. WPD>=200W/m^2) divided by the number of total hours from the MERRA data. Figure 6 shows the availability fraction for southern Africa. A similar pattern emerges from this measure that we have seen before, where there is low availability in the northeastern section of the map. In fact, the majority of this region has availability close to zero, meaning that there are basically no hours with available wind power. Three regions with good availability stand out: Kenya with wind power available around half of the total time; central Tanzania with wind power available between one third and one half; and southwestern South Africa with power available between one fourth and one third of the total time.

The next measure of reliability we have calculated is wind power episode lengths. Here, a wind power episode is defined as a period of time where wind power is usable for consecutive hours. Each of these wind power episodes is found and the number of consecutive hours is recorded. Figure 7 shows the mean (left) and median (right) of the wind power episode lengths. We see that central Kenya has wind power episodes around 20 hours long on average, central Tanzania around 8 to 15, and southwestern South Africa around 8 to 13 hours. Unsurprisingly, the wind power episode lengths appear to be predominantly skewed towards lower values, similar to WPD, although less so. For example, the difference in the median and mean in central Tanzania is about two hours while in southwestern South Africa the difference is closer to three or four hours.

3.4 Changes over different time scales

Since wind speed is driven largely by various climatic states, wind power potential can vary somewhat consistently over the seasonal and diurnal cycles, among others. For this part of the study, we will focus on the Republic of South Africa as an example. First, using the same WPD threshold of 200 W/m^2, we calculate a binary time series representing an hour with either unusable (i.e. less than the threshold) or usable (i.e. greater than the threshold) wind power. Then, we calculate the total number of grids in South Africa with usable power and divide it by the total number of grids in South Africa. From this calculation, we estimate the fraction of grids with power, where a value of one means that all of the grids have power, a value of 0.5 means half of the grids have power, etc. Now we have a single 31-year time series and can make claims on how the wind power potential changes over various time scales. Box and whisker plots showing the distributions over each of the 31 years are shown in Figure 8. We again see that the distributions are skewed toward lower values with a central

tendency around 0.2 and a very long tail reaching toward 1. The 75th percentile, represented by the top of the box, generally lands on 0.4 and the 25th around 0.05. Figure 9 shows the hourly mean over the 31 years in blue. Notice that the value fluctuates somewhat periodically spanning about 0.4. This fluctuation is the diurnal cycle. For this reason, we applied a 24-hour moving average to the hourly mean, shown in red, to remove the large fluctuations. There is a clear seasonal cycle in wind power usability in South Africa, which peaks around October / November followed by a lull around April. Also notice that the mean value fluctuates from about 0.1 to 0.5 in a typical 24-hour period meaning that the WPD in about 40 per cent of the grids drops below the threshold within the day.

Since the above plot only shows the mean of the fraction of grids with usable power in South Africa, we wanted to get a sense of the how the seasonal pattern is distributed over all of the years. Figure 10 shows the 90th (top grey line), 50th (black), and 10th (bottom grey line) percentiles smoothed with a 168-hour (one week) moving median. In this case, the 90th percentile represents the one-week central tendency of the highest fraction of grids with usable power that could be expected in a 10-year period. Similarly, the 10th percentile would be the lowest expected to occur in a 10-year period. The 90th percentile drops to around 0.2 around April and rises above 0.5 around October and November, while the 10th percentile hits a long peak from November to January slightly below 0.1 and a long six-month lull near zero from the middle of March to the middle of September. The median finds a steady peak near the beginning of October that lasts to the middle of January at around 0.5 and drops close to zero at the beginning of May. As a reference, the electricity demand weekly load (as a fraction of the mean) is shown to illustrate changes in demand over the seasons.

Energy demands also vary daily. Figure 11 shows the distribution of the fraction of grids with usable power in South Africa over a 24-hour day using box and whisker plots, in grey, and the mean annual load, in blue. The plot starts 30 minutes after midnight and ends 30 minutes before, so the average daylight hours can be assumed to be between 6:00 and 18:00, although this does change seasonally. To avoid clutter, outliers are not shown in this plot. Outliers are assumed to be any data point greater than $q_3 + 1.5 (q_3 - q_1)$ or less than $q_1 - 1.5 (q_3 - q_1)$, where q_1 is the 25th percentile and q_3 is the 75th percentile. The end of the grey line, top and bottom, represents these limits. The thick grey line represents q_1 at the bottom and q_3 at the top, and the black dot is the median. The red line, again, shows the mean electricity demand profile across the day. As shown, South Africa has a much higher fraction of grids with power during the day than at night. Just after midnight, most of the grids do not have usable power, with a median around 0.03. Around 3:30 the wind starts to increase above the threshold in many of the grids peaking around 10:00 and dropping down to around 0.1 at 15:30. The daily distribution of grids with power is ideal for matching the morning peak demand but fails to meet the peak demand in the evening, about 20:30. Another interesting feature of this plot is the extremes. During the peak hours around 10:00, the distributions reach the full range of possible values, from zero to 1.

3.5 Wind power density at different altitudes

As wind turbine technology advances, increasing the hub height becomes more economically feasible. In a general sense, WPD increases as hub height increases because the roughness of the earth has less of an effect on the wind speeds. But, as the altitude increases, the density of the air decreases at a rate of about 0.01 per cent per meter. This means that an increase of 100 m would result in a reduction of about 1 per cent of the WPD caused by thinner air. The intermittency could also change at different hub heights. In the following section, we will

explore WPD at various heights. Using EQ3, we can estimate wind speeds at different values of z, then convert these to WPD using EQ1.

Figure 12 shows the median WPD at different altitudes for 80 m and the difference between WPD at 80 m and 150 m. Generally speaking, the median WPD increases with height proportional to the central tendency.

Next, we wanted to see how the episode lengths change as altitude increases. Figure 13 shows the mean episode length at 80 m, then again the differences between the value at 80 m and the value at 100 m, 120 m, and 150 m. Although episode lengths are relatively high in South Africa, the length of available wind power does not seem to increase as much with height as the areas in Kenya or central Tanzania. In fact, the northern part of Zambia shows more promise at higher altitudes than South Africa.

3.6 Mapping the value of interconnection

One proposed method for dealing with wind power intermittency is to connect wind farms that have negatively correlated wind speeds. Then, theoretically, when one farm does not have power, the other does, and vice versa. We wanted to investigate this potential in southern Africa using techniques developed by Gunturu and Schlosser (2012).

Anti-coincidence

Here we take the full time series of WPD for every grid point in southern Africa and convert it to a binary dataset, where zeros represent unusable WPD, less than 200 W/m^2, and ones represent usable WPD, greater than 200 W/m^2. For every grid, we look at the surrounding grids in a fixed window and determine that grid's 'score.' This score represents a measure of how useful it would be to interconnect wind farms with the surrounding grids. We have decided to use a window of 19 by 19 grids, as shown in Figure 15. This represents a box that is 10 grids in each direction from the point R. For each grid in this box, the binary values are compared between the point of interest, R, and the surrounding grids, P. A count is made whenever there is wind power at one of the two points and not at the other. If the count is at least half of the total time series, the grid is said to be 'anti-coincident' to the reference, R. The number of grids in the window that meet the anti-coincident criteria are counted and that is the score given to R.

A map showing the anti-coincidence score is shown in Figure 15 for WPD at 80 m, and the other heights: 100 m, 120 m, and 150 m are shown as the difference from the score at 80 m. Note for any grid that is at least 10 grids from the edge, the total number of grids in the window is 360*(19*19 - 1), so a value of 72 means that 20 per cent of the surrounding grids are anti-coincident. The size of the grid box is shown in the northwestern area of each map in Figure 15 as reference.

For the majority of southern Africa, the anti-coincidence score is zero. This is not surprising in the Congo area because the WPD is very low, but it is surprising in Zambia and Zimbabwe where there are some regions of mild potential. Also, it is surprising that central Tanzania is so low, except for a few grids of high anti-coincidence. Another interesting feature of the map at 80 m is the high score along the coast of Namibia and South Africa. This is likely caused by characteristically different wind patterns in the offshore grids compared to the wind patterns inland. From a national planning perspective, this finding could imply that it would be a good investment to match each onshore wind farm with an offshore wind farm,

even though offshore wind farms are more expensive to build. The anti-coincident score also changes considerably for different altitudes. In most of southern Africa the score increases as height increases, especially eastern Africa and the northern coast of Namibia. But there seems to be a dividing line at the southern part of South Africa where the anti-coincidence score decreases with height, likely because the wind in the land grids starts to behave similar to the wind in the ocean grids nearby.

Null anti-coincidence

Gunturu and Schlosser (2011) also used a relaxed criterion to characterize the value of interconnection that emphasizes the instances of unusable power at R. Like in the measure of anti-coincidence, the two binary time series that represent usable and unusable power at R and P are compared. Except, in this measure, only the instances when there is unusable power at R are considered. Every hour where there is usable power at P and unusable power at R are counted. If this count is at least greater than the total number of hours of unusable power at R, the grid, P, is considered to be 'null anti-coincident' to the grid, R. These grids are counted and the total count represents the null anti-coincidence score. Figure 16 shows the schematic diagram for null anti-coincidence.

Since the criteria for null anti-coincidence is somewhat relaxed as compared to the anti-coincidence criteria, we expect a higher null anti-coincidence score. Figure 17 shows the score at different hub heights. The values are highest in eastern Botswana, central Tanzania, and a large area in western Angola. South Africa shows a fairly low null anti-coincidence score, especially in the west where there is a high wind power potential. Another interesting feature of these maps is that the score never increases with hub height in southern Africa. The decreases are largest in Namibia and the cluster near the South Africa-Botswana-Zimbabwe borders.

Correlation with nearby grids

Here we take a different approach to further our exploration of the value of interconnection in southern Africa. In the previous approach, a threshold is assumed in order to transform the dataset into a binary sequence. In order to avoid assuming a threshold, we calculate a Spearman rank correlation. Similar to the anti-coincidence score, we find the rank correlation of each point with the reference in the moving window and take an average of the rank correlations. Figure 18, shows these window-averaged rank correlations for southern Africa. In this case, a point with a negative value suggests that the time series at the point is negatively correlated with the points around it in the 19 by 19 window. Therefore a negative value implies high interconnection value and a positive value implies low interconnection value. Here we see a clear separation between most of South Africa, where the rank correlations are dominantly positive, and the rest of southern Africa, where the rank correlation is mostly negative.

Principal component analysis

In the following, we investigate the variance of the hourly wind speeds in southern Africa using Principal Component Analysis (PCA). PCA reduces the dimensionality of a set of data into vectors of dominating variance, where the first principal component explains the most variance; the second explains the second most, etc. Figure 19 shows the coefficients, or eigenvectors, of the first eight principal components. The first principal component explains 19 per cent of the variance; the second explains 7 per cent, and so on. There are 4,675

principal components total, in this case. The first eight principal components capture over half of the total variance. The areas in the maps with similar coefficient values exhibit the pattern captured in that particular principal component. Basically, the red areas in the maps are out of phase with the blue areas and the percentage value can be thought of as a measure of importance of that principal component. The first principal component shows positive values over land and some negative values in the Atlantic Ocean. This map shows that WPD onshore is negatively correlated with WPD in the Atlantic Ocean. When we look at this principal component in time series, we see a strong 24-hour cycle as well as a seasonal cycle. The second principal component has captured variance that shows that South Africa is in phase with the ocean around it and out of phase with the rest of southern Africa. This second principal component is likely the variance that was captured in the rank correlation map shown previously. Principal components 3 through 7 display interesting features in the Atlantic Ocean that were likely captured in the anti-coincidence score.

Since the grid domain affects the resulting PCA, we decided to narrow the domain to onshore grids in the Republic of South Africa. We also decided to use the Vestas V80 2000/80 2MW wind turbine. The power curve for this turbine is shown in Figure 1. Figure 20 shows the eigenvalues from this analysis for the first eight principal components. The percent of variance represented is shown in parenthesis. Of course, the PCA with a narrower domain is able to explain more variance in fewer principal components. In this case, the first four principal components contain over 60 per cent of the variance. The first principal component, which explains 38 per cent of the capacity factor variance, is all in phase, especially the area in the southwest where most of the wind power potential resides. This result is not ideal for interconnection. In the remaining principal components we see distinct regions that are either in-phase or out-of-phase. Principal components 2, 4, 5, and 6 suggest that the area along the coast in the Eastern Cape province is out-of-phase with areas in the Western Cape and Northern Cape. These being out-of-phase suggest interconnection value; although, summing the variance explained by these principal components only gets us 24 per cent—still much less than the first principal component.

4   Closing remarks

Using the MERRA data, we have mapped and identified areas of high and low wind resource potential. Based on this analysis, South Africa has moderate to high potential for wind power harvesting, especially in the west and south near the coast. Further, we find that although South Africa's mean WPD is close to that of central Tanzania, wind resource in central Tanzania is more reliable. The conclusion was not obvious in the map of mean wind speed or mean WPD, but in using other measures like median, availability, and wind power episode lengths. In order to understand how South Africa's wind power potential changes over various time scales, we plot the percentage of area with usable wind power based on a threshold of WPD. South Africa's potential varies over the year, with higher potential in the summer and lower potential in the winter. We also find that a larger area of South Africa has usable WPD during the day than at night. In order to assess the value of interconnection, a suggested method to reduce intermittent output, we present various measures. Depending on the measure, different results are found. In the final measure, we show maps of dominating variances and the regions that are contributing, either positively or negatively, by use of a PCA.

References

Adrian, G., and Fiedler, F. (1991). 'Simulation of Unstationary Wind and Temperature Fields over Complex Terrain and Comparison with Observations'. *Beiträge zur Physik der Atmosphäre*, 64:27–48.

Adrian, G. (1995). 'On Similarity Laws in Regional Climatology'. *Archiv für Meteorologie, Geophysik und Bioklimatologie Serie A*, 55(3–4), 223–234.

Alton, T., Arndt, C., Davies, R., Hartley, F., Makrelov, K., Thurlow, J., Ubogu, D. (2012). 'The Economic Implications of Introducing Carbon Taxes in South Africa'. UNU-WIDER Working Paper No. 2012/46.

Cavallo, A.J., Hock, S.M., Smith, D.R. (1993). 'Wind Energy: Resources, Systems, and Regional Strategies'. In T. B Johansson. H. Kelly, A.K.N. Reddy, R.H. Williams (eds), *Renewable Energy - Sources for Fuel and Electricity*. Island Press.

Department of Environmental Affairs (DEA) (2011). 'South Africa's Second National Communication under the United Nations Framework Convention on Climate Change'. Republic of South Africa, Pretoria: DEA.

Diab R. (1995). 'Wind Atlas of South Africa'. Pretoria: Department of Minerals and Energy.

Department of Energy (DOE) (2011). 'Integrated Resource Plan for Electricity: 2010– 2030 (Revision 2 Final Report)'. Pretoria: Republic of South Africa.

Elliott, D.L., Holladay, C.G., Barchet, W.R., Foote, H.P., and Sandusky, W.F. (1987). Wind Energy Resource Atlas of the United States. *NASA STI/Recon Technical Report N*, 87: 24819.

Elliott, D.L., Wendell, L.L., and Gower, G.L. (1991). 'An Assessment of the Available Windy Land Area and Wind Energy Potential in the Contiguous United States. Pacific Northwest Lab., Richland, WA (United States).

Eskin, N., Artar, H., and Tolun, S. (2008). 'Wind Energy Potential of Gökçeada Island in Turkey. *Renewable and Sustainable Energy Reviews*, 12(3): 839–851.

Eskom (2012). Available at: http://www.eskom.co.za (accessed October 2012).

Gunturu, U. B., and Schlosser, C.A. (2011). 'Characterization of Wind Power Resource in the United States and its Intermittency.' *MIT Joint Program on the Science and Policy of Global Change*, Cambridge, 24(14), 3624–3648.

Gunturu, U.B., and Schlosser, C.A. (2012). 'Characterization of Wind Power Resource in the United States. *Atmospheric Chemistry and Physics Discussions*.

Gustavson, M.R. (1979). 'Limits to Wind Power Utilization'. *Science*, 204(4388): 13.

Hagemann, K. (2003). 'Validation of Mesoscale Modeling Data for Wind Resource Assessments'. BSc Honours Thesis. Cape Town: Department of Environmental and Geographical Science, University of Cape Town.

Hagemann, K. (2008). 'Mesoscale Wind Atlas of South Africa'. PhD Dissertation. Cape Town: University of Cape Town.

He, Y., Monahan, A.H., Jones, C.G., Dai, A., Biner, S., Caya, D., and Winger, K. (2010): 'Probability Distributions of Land Surface Wind Speeds over North America'. *Journal of Geophysical Research*, 115(D4): D04103.

Jaramillo, O.A., and Borja, M.A. (2004). 'Wind Speed Analysis in La Ventosa, Mexico: A Bimodal Probability Distribution Case'. *Renewable Energy*, 29(10): 1613–1630.

Landberg, L., Myllerup, L., Rathmann, O., Petersen, E.L., Jørgensen, B.H., Badger, J., and Mortensen, N.G. (2003). 'Wind Resource Estimation? An Overview.' *Wind Energy*, 6(3): 261–271.

Morrissey, M., Cook, W., and Greene, J. (2010). 'An Improved Method for Estimating the Wind Power Density Distribution Function'. *Journal of Atmospheric and Oceanic Technology*, 27(7): 1153–1164.

Peterson, E.L., Mortensen, N.G., Landberg, L., Hojstrup, J., and Frank, H. P. (1997). 'Wind Power Meteorology'. Roskilde: Riso National Laboratory.

Pryor, S.C., and Barthelmie, R.J. (2010). 'Climate Change Impacts on Wind Energy: A Review'. *Renewable and Sustainable Energy Reviews*, 14(1): 430–437.

Republic of South Africa (RSA) (2010). *Reducing Greenhouse Gas Emissions: The Carbon Tax Option.* Pretoria: National Treasury, Government of the Republic of South Africa.

Rienecker, M.M., Suarez, M.J., Gelaro, R., Todling, R., Bacmeister, J., Liu, E., Bosilovich, M.G., Schubert, S.D., Takacs, L., Kim, G.-K., Bloom, S., Chen, J., Collins, D., Conaty, A., da Silva, A., Gu, W., Joiner, J., Koster, R.D., Lucchesi, R., Molod, A., Owens, T., Pawson, S., Pegion, P., Redder, C.R., Reichle, R., Robertson, F.R., Ruddick, A.G., Sienkiewicz, M., and Woollen, J. (2011). 'MERRA: NASA's Modern-Era Retrospective Analysis for Research and Applications.' *Journal of Climate*, 24(14), 3624–3648.

Sailor, D. J., Smith, M., and Hart, M. (2008). 'Climate Change Implications for Wind Power Resources in the Northwest United States. *Renewable Energy* 33: 2393–2406.

Southern Africa Power Pool (SAPP) (2010). 'SAPP Statistics 2010'. Available at: http://www.sapp.co.zw/docs/R9%20-%20SAPP%20Statistics%20-%202010.pdf

Southern Africa Power Pool (SAPP) (2012). 'Annual Report 2012'. Available at: http://www.sapp.co.zw/docs/SAPP%202012%20annual%20report.pdf

Savannah Environmental (2007). 'Final Scoping Report: Proposed Wind Energy Facility and Associated Infrastructure, Western Cape Province'. Report prepared for Eskom Holdings Limited.

Schwartz, M., and Elliot, D. (2005). 'Towards a Wind Energy Climatology at Advanced Turbine Hub-Heights'. Preprint, 15th Conference on Applied Climatology, Savannah, GA, American Meteorological Society.

Stull, R.B. (1991). *An Introduction to Boundary Layer Meteorology*, Volume 13. Dodrecht: Kluwer Academic Publishers.

Szewczuk, S., and Prinsloo, E. (2010). 'Wind Atlas for South Africa (WASA)'. Quaternary Real and Relevant Conference, Available at: http://www.sawea.org.za/images/stories/SAWEA%20docs/WASA_SAWEP_2010.pdf (accessed 2 May 2012).

Troen, I., and Petersen, E., (1987). 'European Wind Atlas'. Roskilde: Riso National Laboratory.

Tuller, S.E., and Brett, A.C. (1984). 'The Characteristics of Wind Velocity That Favor the Fitting of a Weibull Distribution in Wind Speed Analysis'. *Journal of Applied Meteorology*, 23: 124–134.

Ucar, A., and Balo, F. (2009). 'Investigation of Wind Characteristics and Assessment of Wind-Generation Potentiality in Uludag-Bursa, Turkey'. *Applied Energy*, 86(3): 333–339.

Wind Atlas for South Africa (WASA) (2012). Available at: http://www.wasaproject.info (accessed 2 May 2012).

Wilson, D., and Adams, I. (2006). 'Review of Security of Supply in South Africa'. A Report to the Department of Public Enterprise.

Zaharim, A., Razali, A.M., Abidin R.Z., and Sopian, K. (2009). 'Fitting of Statistical Distributions to Wind Speed Data in Malaysia'. *European Journal of Scientific Research*, 26(1): 6–12.
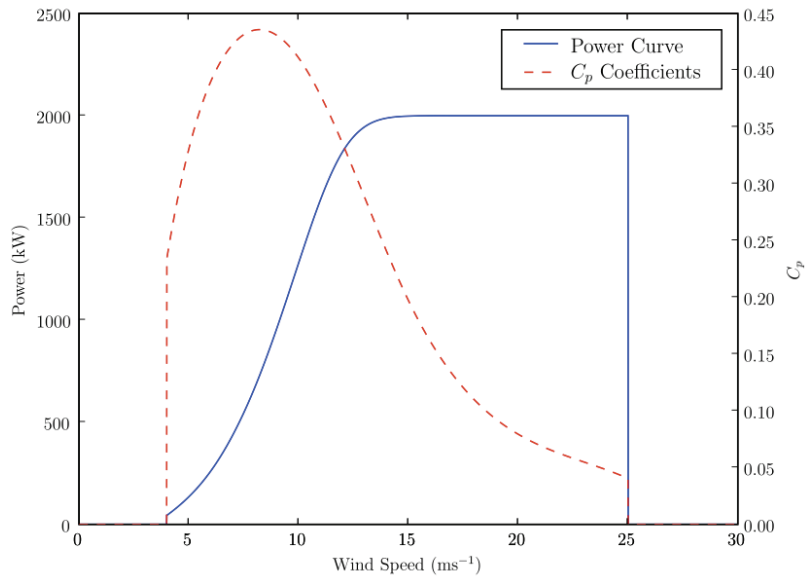
Figure 1: Power curve and C_p coefficients for a Vestas V80 2000/80 2MW turbine at 1.225km/m^3

Source: Hagemann (2008).
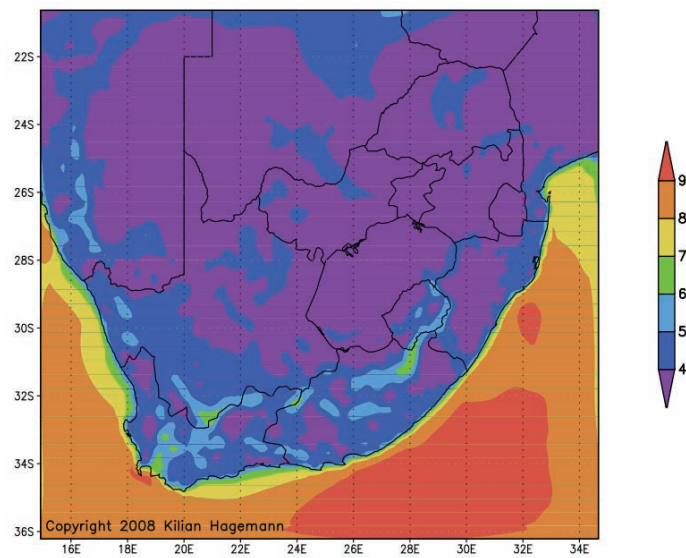
Figure 2: Average annual wind speed 10 m above ground

Source: Hagemann (2008).
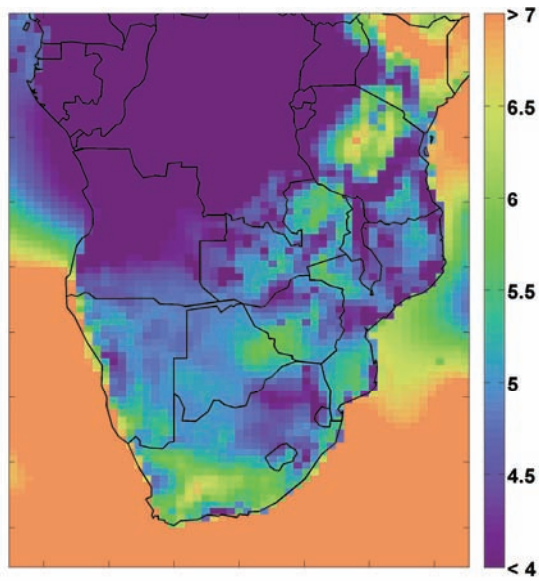
Figure 3: Mean wind speed (m/s) at 50 m for southern Africa

Source: authors' creation.
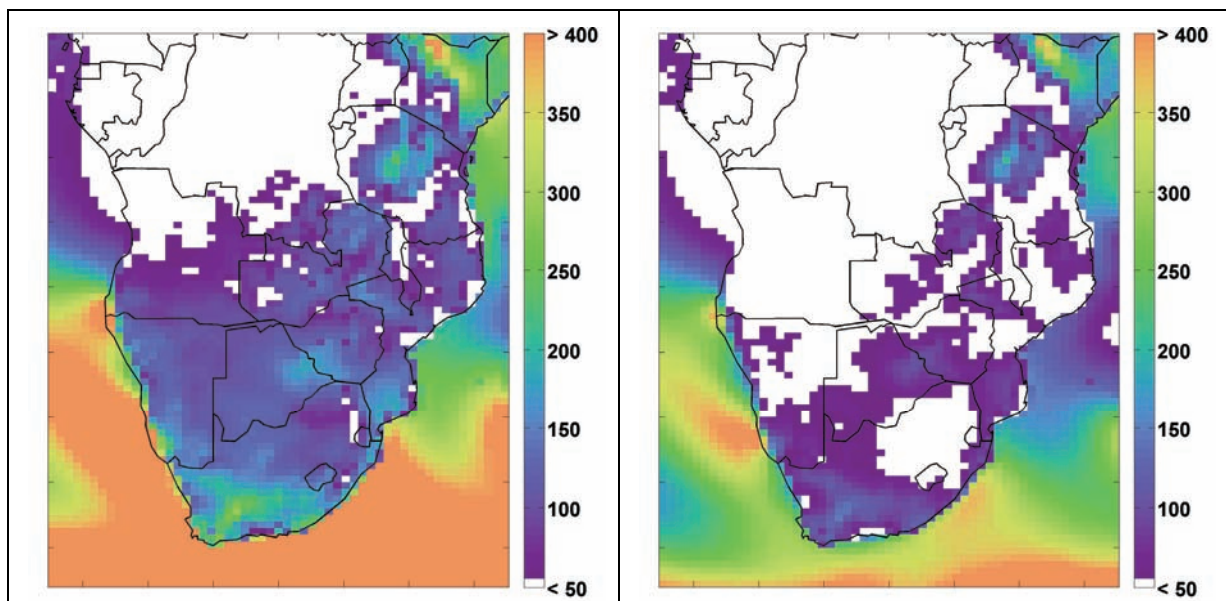
Figure 4: Mean (left) and median (right) wind power density (W/m^2)

Source: authors' creation.
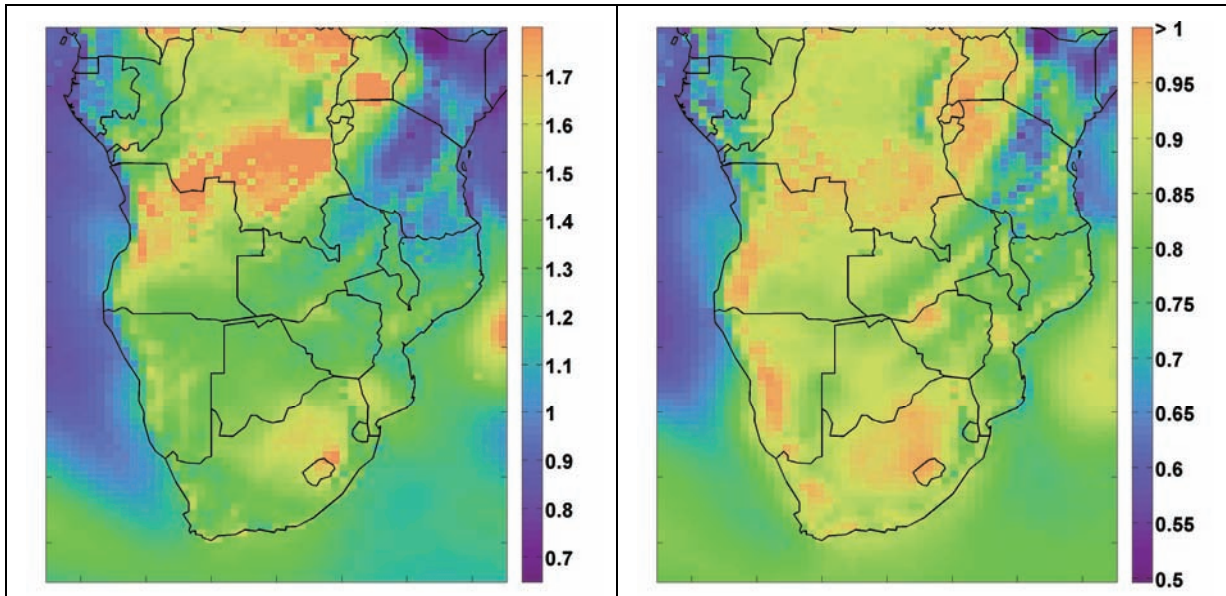
Figure 5: Coefficient of variance (left) and the robust coefficient of variance (right) of WPD

Source: authors' creation.
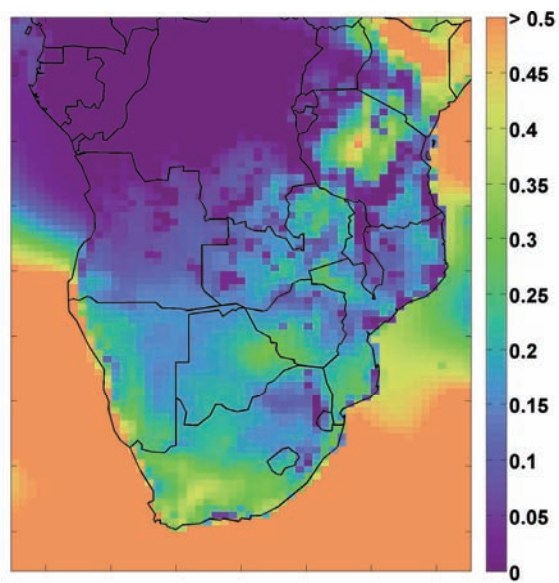
Figure 6: Availability of WPD at 50 m

Source: authors' creation.
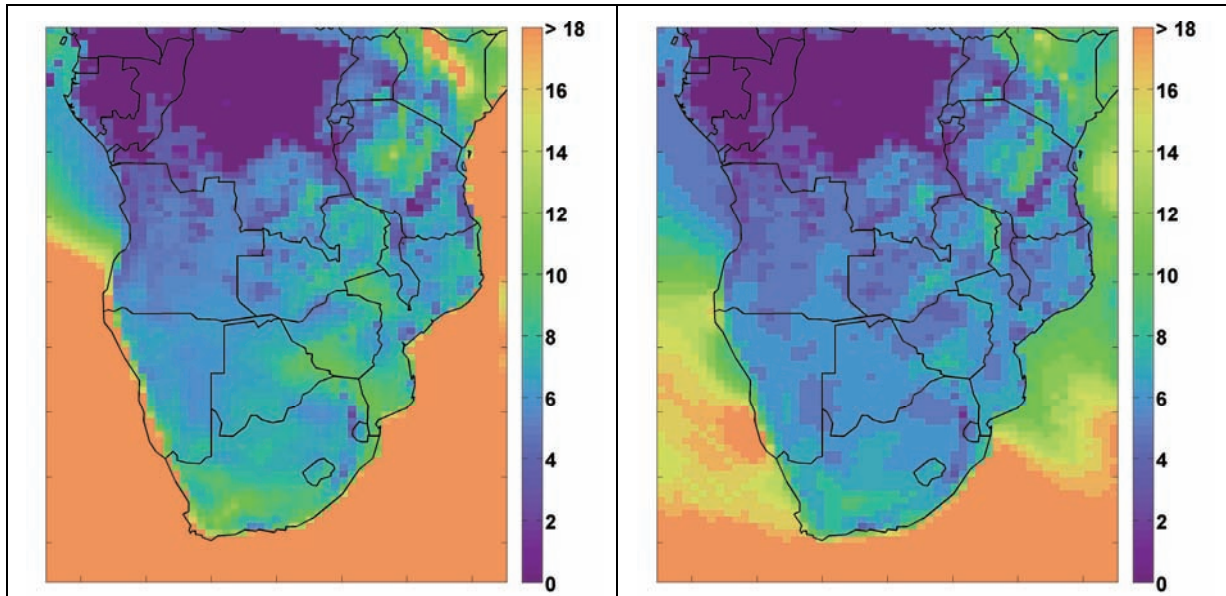
Figure 7: Mean (left) and median (right) of wind power density episode lengths at 50 m hub height

Source: authors' creation.
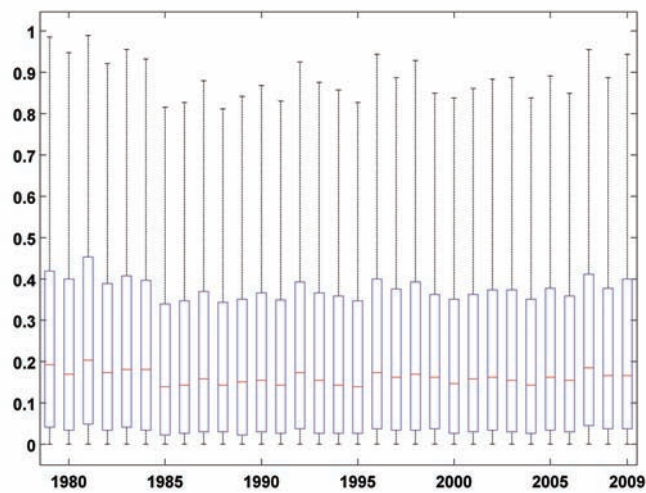
Figure 8: Distributions of the fraction of grids with usable WPD for each year of the MERRA data

Source: authors' creation.

17
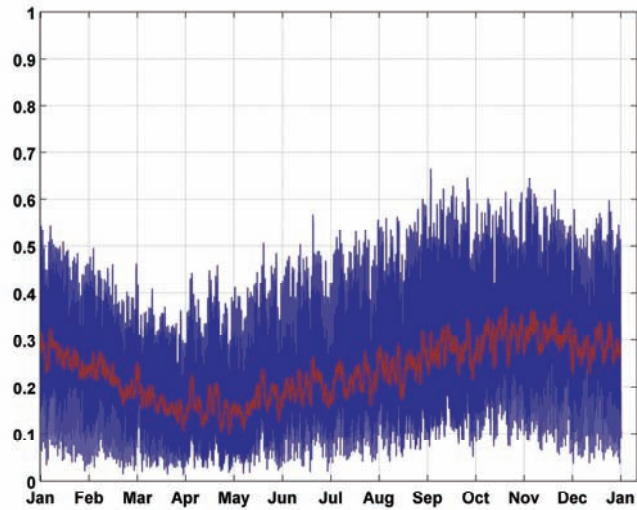
Figure 9: Hourly mean fraction of grids with usable power over the calendar year

Note: calculated over 1979–2009 in blue and with a 24-hour moving mean in red.

Source: authors' creation.
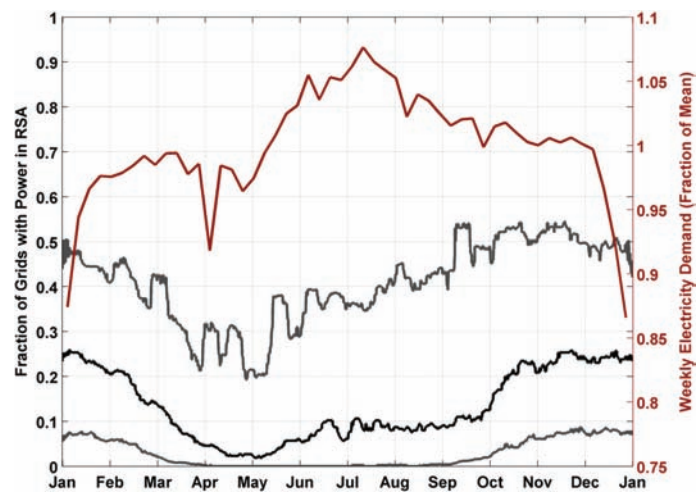
Figure 10: Seasonal distribution of the fraction of grids with usable WPD in South Africa

Source: authors' creation.
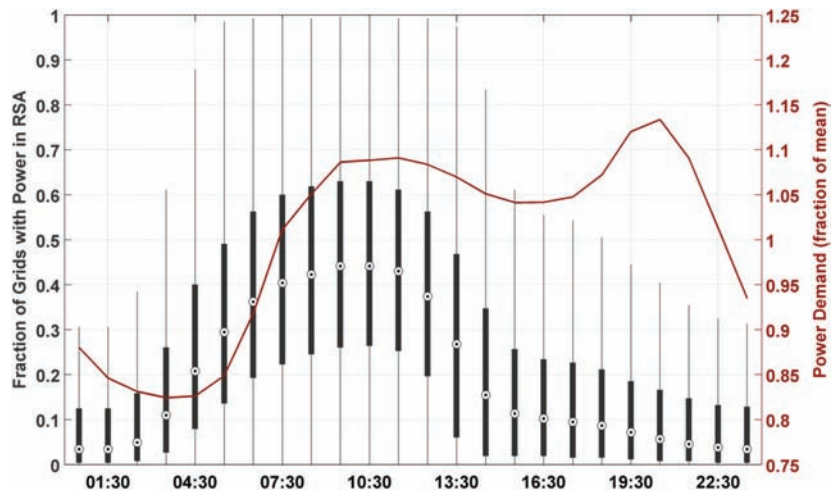
Figure 11: Diurnal distribution of the fraction of grids with usable WPD in South Africa

Source: authors' creation.
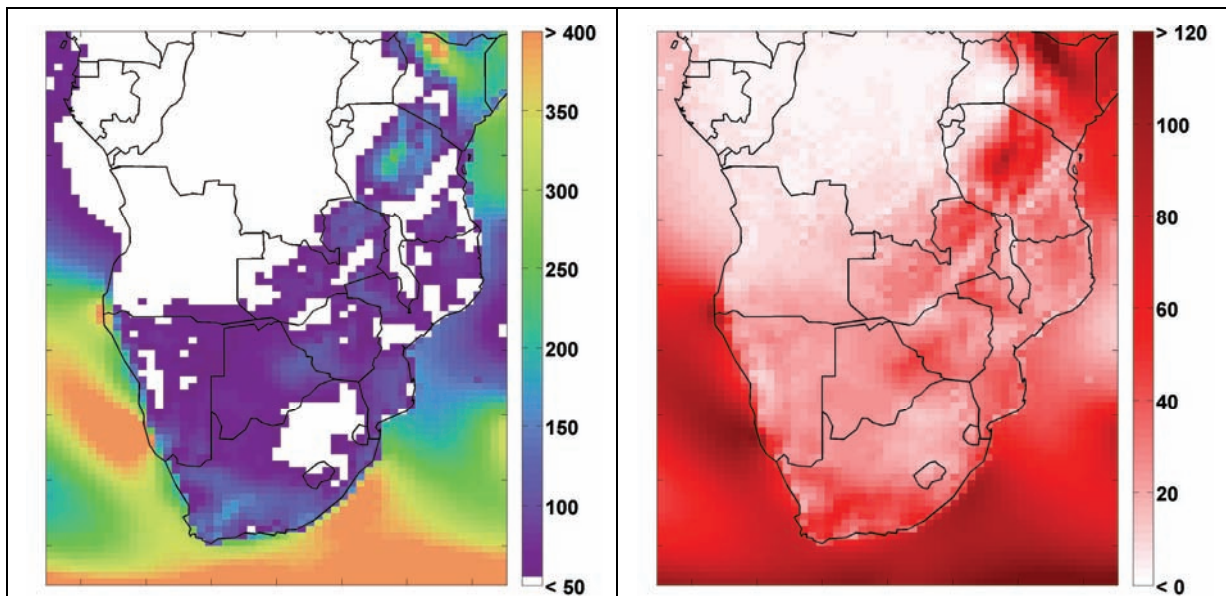
Figure 12: Median wind power density (W/m^2) at different hub heights

Note: 80m (left) and the difference between 150m and 80m (right).

Source: authors' creation.
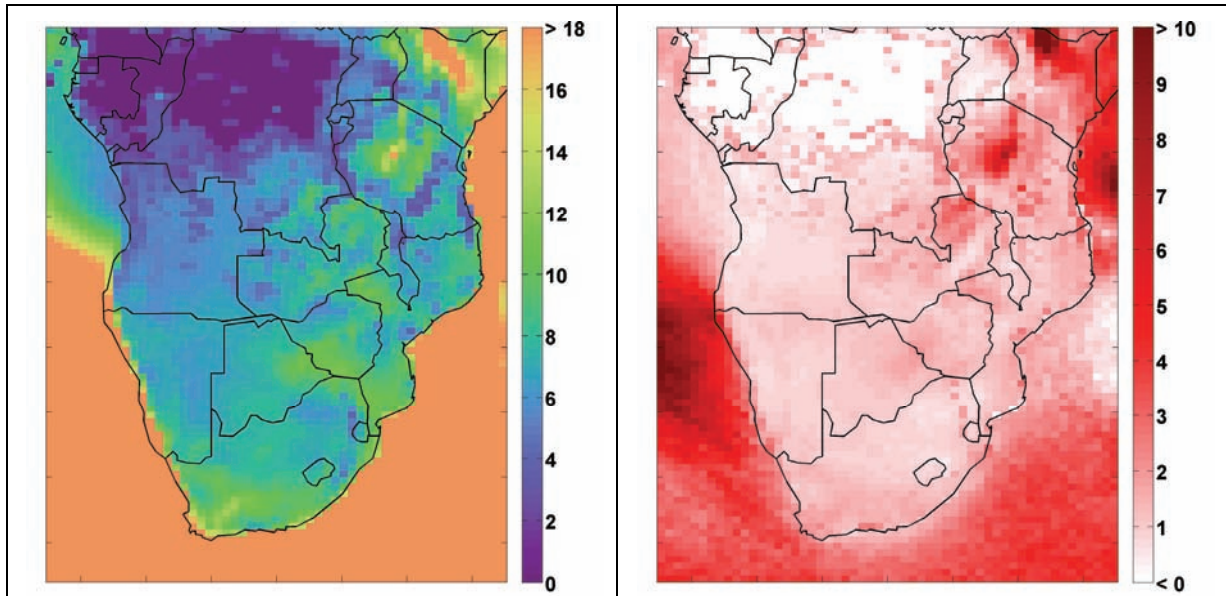
Figure 13: Mean of wind power episode length (hours) at different hub heights

Note: 80m (left) and difference between 150m and 80m (right).
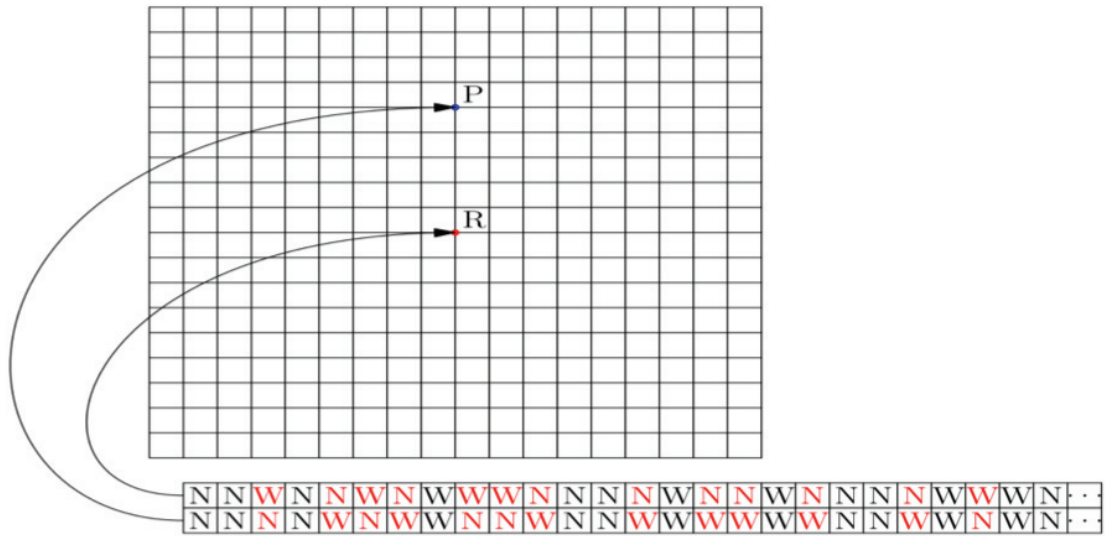
Source: authors' creation.

Figure 14: Anti-coincidence schematic diagram

Source: authors' creation.
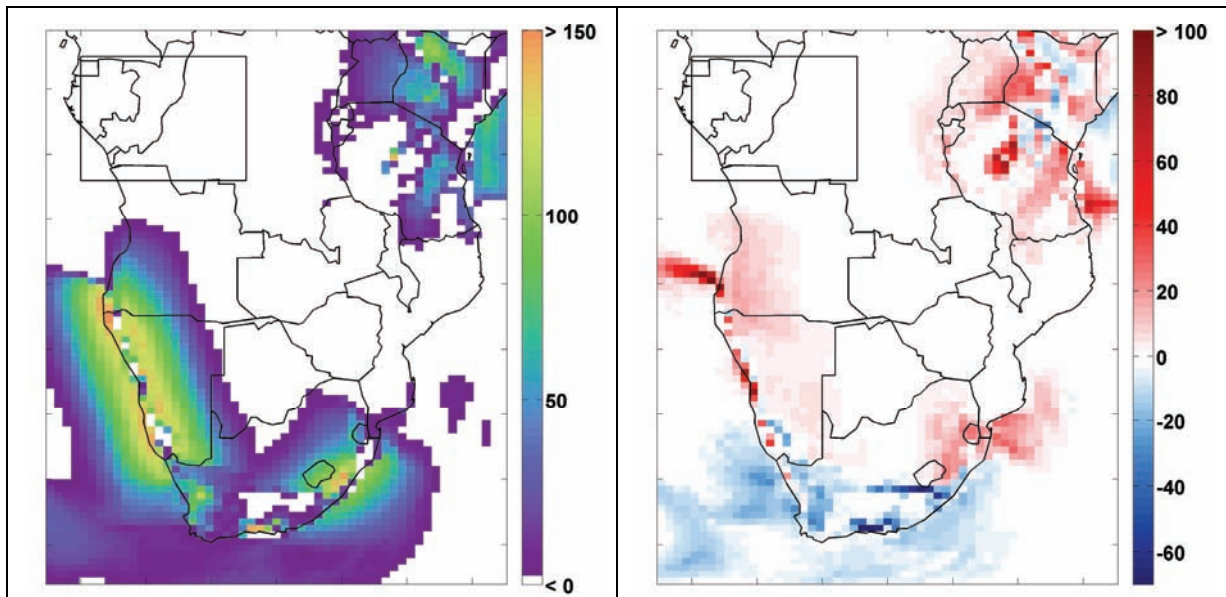
Figure 15: Anti-coincidence score at different hub heights

Note: 80m (top left); difference between 100m and 80m (top right); difference between 120m and 80m (bottom left); difference between 150m and 80m (bottom right).
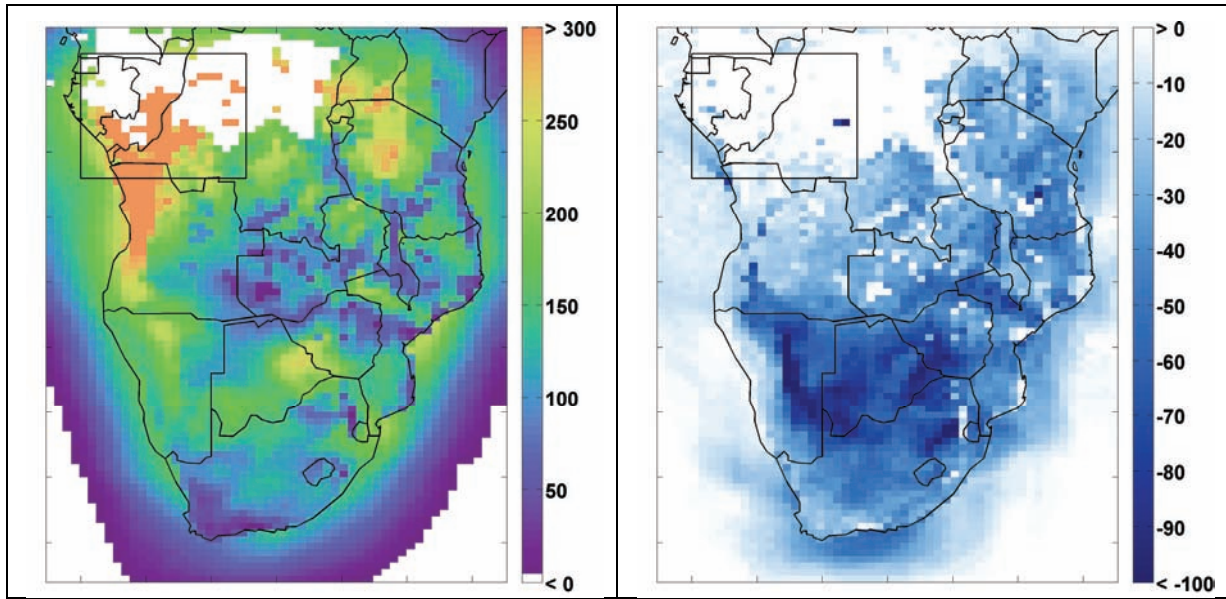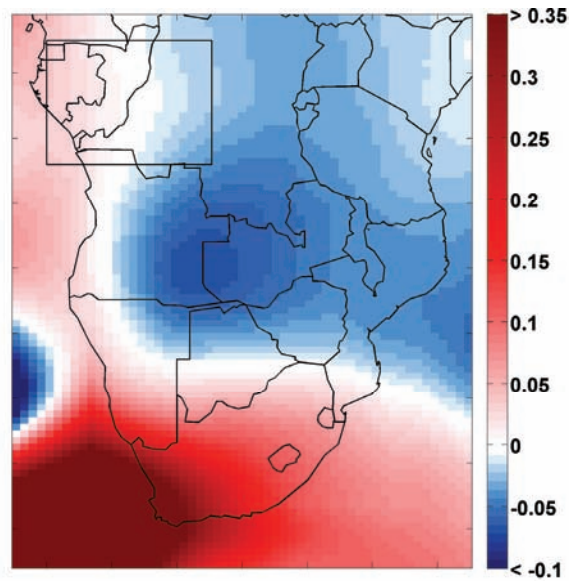
Source: authors' creation.

Figure 16: Null anti-coincidence schematic diagram

Source: authors' creation.

Figure 17: Null anti-coincidence score at different hub heights

Note: 80m (top left); difference between 100m and 80m (top right); difference between 120m and 80m (bottom left); difference between 150m and 80m (bottom right)

Source: authors' creation.

Figure 18: Geographic variation of the mean rank correlation with nearby grids
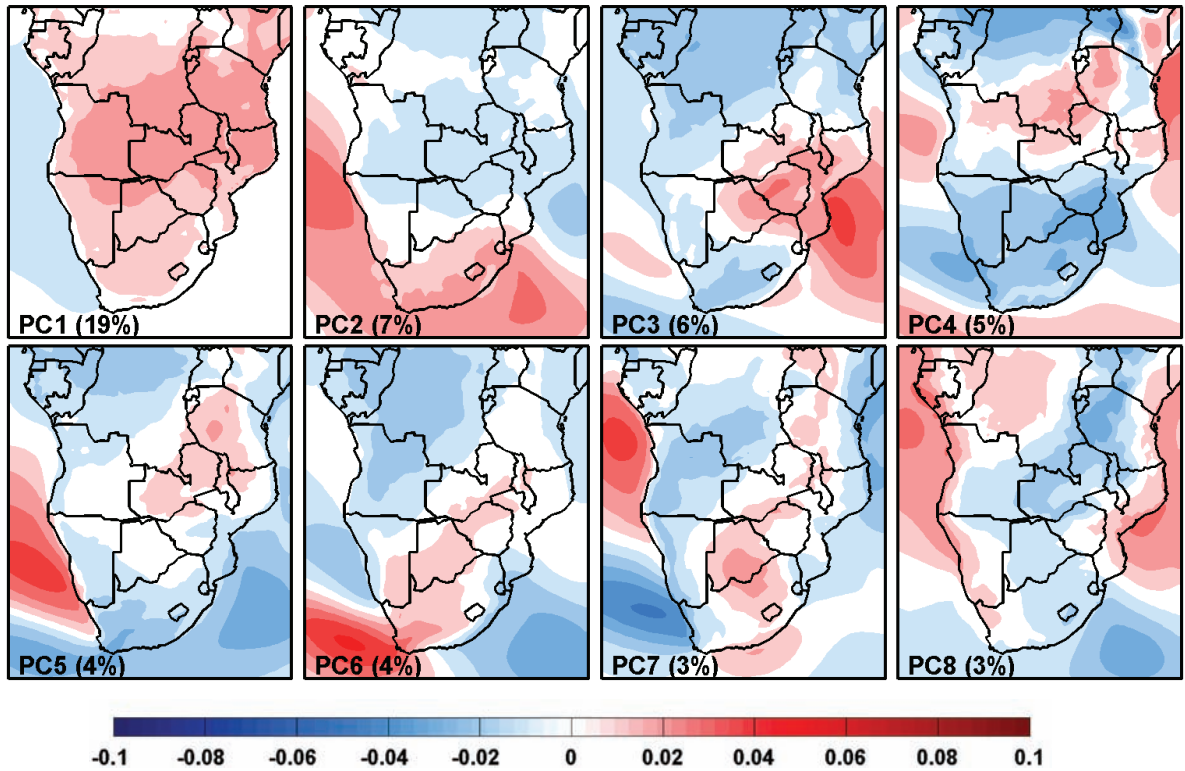
Source: authors' creation.

Figure 19: The first eight principal component coefficients from the PCA of hourly WPD dataset over southern Africa.

Note: The values in parentheses are the percentage of variance explained by that principal component.
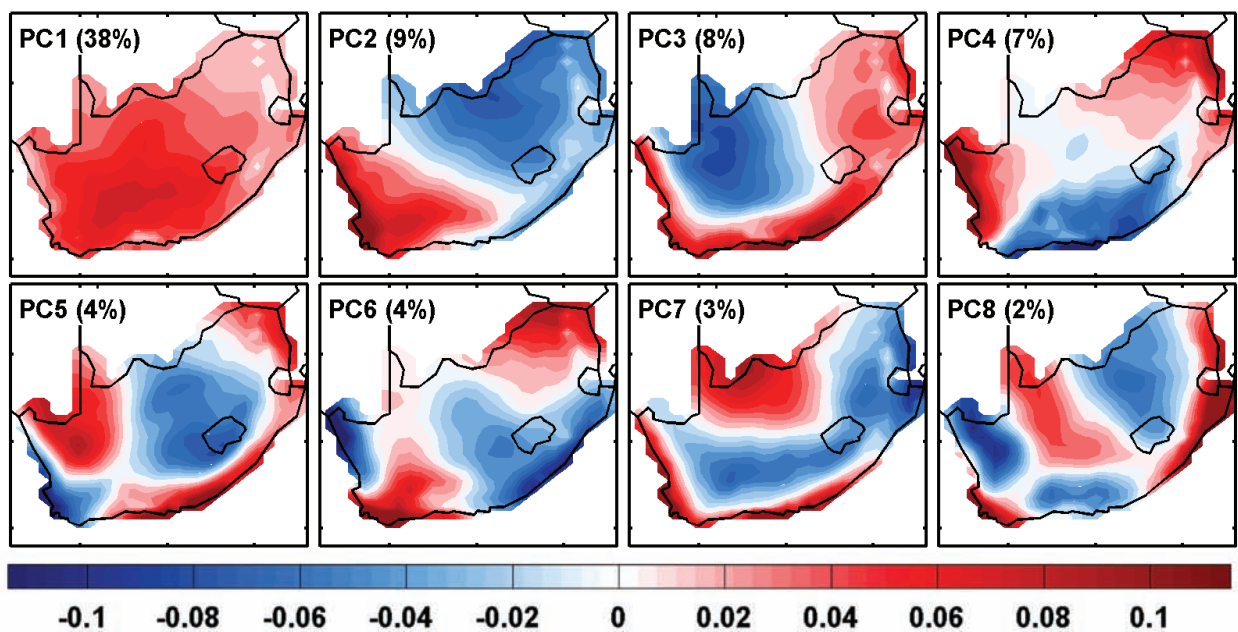
Source: authors' creation.

Figure 20: Geographic variation of eigenvalues from the first eight Principal Components performed on the onshore capacity factor in South Africa

Source: authors' creation.